

# ALGEBRAIC INTERPRETATION OF COMPOSITION PHASE CLASSIFICATION CRITERIA FOR CCSEM.

Peter N. Slater, M. Bret Abbott, and John N. Harb  
 Department of Chemical Engineering and Advanced Combustion Engineering Research Center  
 Brigham Young University  
 Provo, UT 84602

Keywords: CCSEM, Fly Ash, Classification

## INTRODUCTION

Data from computer controlled scanning electron microscopy (CCSEM) are typically interpreted by grouping particles into bins based on their elemental compositions. Some of the bins correspond to well-defined mineralogical species or phases with known properties. Other bins are defined for convenience so that similar particles can be grouped together. Experience has shown that it is difficult to predict *a priori* what phases will be determined in an analysis; this is particularly true in the case of fly ash samples which are largely amorphous at combustion temperatures. Often a large number fraction of the analyzed particles do not fit any of the predefined phases and are classified as unknown. In such cases, it is difficult to interpret the analysis results since nothing is known about a large fraction of the sample. It is desirable then to have a means of extracting some sort of composition information from the unclassifiable particles. This paper addresses the problem of defining new bins to describe particles which do not fit into the predefined classifications using an algebraic formulation of the criteria.

## METHOD

CCSEM reports particle compositions as n-dimensional vectors, where n is the number of elements analyzed. Typically, n is equal to twelve and the elements are Na, Mg, Al, Si, P, S, Cl, K, Ca, Ti, Fe, and Ba. To determine whether or not a given composition belongs to a phase, numerical tests or criteria are applied. These tests are linear inequalities, e.g.,  $Si + Al \leq 80$ , or ratios, e.g.  $Si/Al \leq 2$ , which can be expressed as linear inequalities. Therefore, the test for membership in a phase can be written as a system of linear inequalities. Using matrix notation, the test can be written  $Ax \leq b$ , where the rows in the matrix A and the vector b correspond with the individual criteria.

Consider for example, a simple system with two elements, X and Y, and two phases, A and B with constraints as follows:

Phase A	Phase B
$x \leq 40$	$x \geq 80$
$y \leq 40$	$y \leq 40$
	$x + y \leq 100$

It is implicitly assumed that compositions are limited by zero below and by one hundred percent above. The algebraic forms for these two phases would be:

Phase A	Phase B
$\begin{bmatrix} 1 & 0 \\ 0 & 1 \end{bmatrix} \begin{bmatrix} x \\ y \end{bmatrix} \leq \begin{bmatrix} 40 \\ 40 \end{bmatrix}$	$\begin{bmatrix} -1 & 0 \\ 0 & 1 \\ 1 & 1 \end{bmatrix} \begin{bmatrix} x \\ y \end{bmatrix} \leq \begin{bmatrix} -80 \\ 20 \\ 100 \end{bmatrix}$

Note that the sign of the first constraint for phase B has been changed so that it could be written in the less than or equal to form. The phases can also be represented as regions in the x-y plane, as illustrated in Figure 1. Any composition (x,y) falling within the square region at the lower left would be classified as phase A. Likewise, phase B would comprise any composition falling within the triangular region at upper right. Any other composition, such as the points indicated in the figure, would be unclassified.

The unclassifiable points in Fig. 1 appear in two distinct clusters. One is nearer to phase A and the other is nearer to phase B. The observation that unknown particles tend to appear in clusters when plotted in this fashion and that a cluster would of necessity lie closest to one phase is the basis for the algebraic classification scheme: find the distance to each of the defined phases and then group the composition with the phase having the shortest distance.

Finding the distance from a point to a given phase is an optimization problem called a quadratic program. The quadratic objective function is the square of the Euclidean distance from the composition to a composition that meets the phase's criteria. By minimizing this objective function subject to the criteria, the composition within the phase closest to the given composition is determined. Examination of the resulting groupings of unknown compositions from a complete CCSEM analysis reveals trends and clusters of points which can be used to define new phases. This classification scheme is shown in Fig. 2.

The algorithm has been implemented using a sparse matrix data structure to minimize the memory and computational requirements. Several thousand known compositions can be classified

in minutes on a 75MHz Pentium computer. Using a numerical Sequential Quadratic Programming (SQP) algorithm to solve the quadratic programs on an HP 9000/755 workstation, several thousand unknown compositions can be classified in about an hour. The number of optimizations required is  $m \cdot p$ , where  $m$  is the number of unknown particles and  $p$  is the number of known phases. Given this dependence, it has proven wise to start with a relatively small number of particles, several hundred rather than several thousand, and define new phases based on the initial results before proceeding to the complete data set. This dramatically reduces the number of optimizations.

## RESULTS AND DISCUSSION

The method has been applied to the analysis of ash derived from Pittsburgh #8, an eastern subbituminous coal, and ash from Black Thunder, a western subbituminous coal from the Anderson seam of the Powder River Basin. ASTM ash analyses of the elemental oxides from both coals are presented in Table 1. Note the low-rank Black Thunder contains a great deal of organically bound calcium and relatively few discrete mineral grains. Its ash, therefore, is expected to be significantly influenced by the organically bound constituents. The inorganic content of Pittsburgh #8, however, is primarily discrete minerals. The major mineral species found in the Pittsburgh coal are pyrite, quartz, aluminosilicates, potassium aluminosilicates, pyrite, and calcite [1]. The ash of Pittsburgh #8 is controlled by the transformations (coalescence and fragmentation) of the discrete minerals during combustion.

Ash data from both coals were classified using a typical set of phases. This set consisted of 47 well-defined phases [3] and several more loosely-defined aluminosilicate phases. The results of the classification are presented in Table 2. The heavy line separates the loose phases from the phases that were more well-defined. Minor phases have been omitted from the table for brevity. The phase set used is clearly inadequate for characterizing these ashes; 58% of the Black Thunder and 24% of the Pittsburgh #8 particles were unclassifiable. In fact, only 14% of the Black Thunder and 7.54% of the Pittsburgh #8 was classified with the well-characterized bins, and the majority of that was quartz.

In the Pittsburgh #8 ash, 39% of the particles contained five mole percent or more iron. Of these, 19% or nearly half of the iron-bearing particles were unclassifiable. Given the importance of iron in ash deposition behavior, it is essential to know more about its occurrence in the ash than is provided by the this typical phase set.

The algebraic classification scheme was applied to the Black Thunder ash using the 47 well-defined phases. Results are tabulated in Table 3. The quantities are reported in percentage of original particles (classifiable plus unclassifiable). Minor phases (less than 1% of total) have been omitted. Only values for Mg, Al, Si, Fe, and Ca are reported since these five elements were found to be sufficient to characterize the bins. Of course, other elements do play a role in the properties of individual particles and the category as a whole. Their omission in the table does not imply that they should be ignored when the CCSEM analysis is interpreted. The table includes the mean value and standard deviation for each of the elements included.

Using the 47 phases, 85% of the Black Thunder ash particles were unclassifiable. The algebraic classification scheme was able to classify 82% of the particles into eight major phases. The contents of the various bins are distinct from one another, as evidenced by the differences in the means of the major elements which characterize each bin. The "near quartz" category has the highest mean silicon content, 76%. Several bins share the same major elements, but in clearly distinguishable compositions. It is sometimes desirable to further subclassify these bins; preliminary work has shown that classifications based on the ranking of the four most abundant elements in a particle is a good basis for distinguishing composition within a nearest-phase category.

To focus on the distribution of iron in the 24% of the particles that were found unclassifiable, the algorithm was applied to the Pittsburgh #8 ash using the phase set which included the loosely-defined bins. The results for the major iron-containing bins are presented in Table 4. Bins were chosen for inclusion based on the fraction of the total iron-bearing particles they contained; bins with less than one percent have been omitted. It is clear that most of the unclassifiable particles contain iron and that they can be grouped into nine major categories. The means in these categories are distinct, indicating that the algorithm has indeed differentiated the particles.

In most cases, particles did not fit into their nearest phases because they contained too much of a minor constituent. Cutoffs are typically five mole percent. In the "near Fe-Al-Silicate" phase, 44% of the particles contained too much calcium, 32% contained too much potassium, and 18% contained too much sodium. Many particles violated more than one constraint; i.e. they contained too much of two or more elements. Examination of the reasons why particles do not fit the known phases yields insight into both the ash composition and the mechanisms by which it formed.

## CONCLUSIONS

Particle composition classification schemes must be designed to provide meaningful information about specific ash samples due to the variability in the parent fuels and combustion conditions. Using a generic set of phases, large fractions of the particles are often unclassifiable.

The algebraic interpretation of the phase criteria provides a straightforward means of classifying these particles with no assumptions about the dominant elements or the form that the new classifications should take. The classifications thus made provide a number of distinct categories that can be used to characterize the ash.

#### ACKNOWLEDGMENTS

The authors wish to thank David P. Kalmanovitch for his invaluable assistance in formulating the criteria used to identify crystalline phases. Rachel Newsom and Eyas Hmouz undertook the tedious work of translating the phase criteria for use with the algebraic classification program. This work was funded by the U.S. Department of Energy under the University Coal Research Program, Grant No. DE-FG22-93PC93226. Additional funding was provided by the Advanced Combustion Engineering Research Center (ACERC) at Brigham Young University. Funds for ACERC are received from the National Science Foundation, the State of Utah, 42 industrial participants, and the U.S. Department of Energy.

#### REFERENCES

1. Harb, J.N. (1994) Investigation of Mineral Transformations and Ash Deposition During Staged Combustion, Quarterly Progress Report #3, U.S. Department of Energy Contract DE-FG22-93PC93226.
2. Richards, G. H. (1994) Investigation of Mechanisms for the Formation of Fly Ash and Ash Deposits for Two Powder River Basin Coals, Ph.D. Dissertation, Brigham Young University, Provo, UT, 84602.
3. Kalmanovitch, D.P. (1991) Personal Communication

Table 1. Ash Oxide Analyses (SO<sub>3</sub>-free) of Black Thunder and Pittsburgh #8 Coals

Weight % of Ash	Black Thunder [2]	Pittsburgh #8 [1]
SiO <sub>2</sub>	36.7	47.86
Al <sub>2</sub> O <sub>3</sub>	19.7	21.79
Fe <sub>2</sub> O <sub>3</sub>	6.1	18.01
TiO <sub>2</sub>	1.5	1.06
CaO	25.5	6.69
MgO	5.7	1.16
Na <sub>2</sub> O	1.7	0.75
K <sub>2</sub> O	0.4	1.73
P <sub>2</sub> O <sub>5</sub>	1.1	0.37

Table 2. Phase Distribution of Ash Particles

Phase	Black Thunder (% of particles)	Pittsburgh #8 (% of particles)
Quartz	12.38	5.31
Iron Oxide/Carbonate	0.0	2.23
Plagioclase Solution	1.76	0.0
Kaolinite	12.54	35.77
Ca-Al-Silicate	6.2	3.61
Na-Al-Silicate	5.35	1.8
K-Al-Silicate	1.44	8.67
Fe-Al-Silicate	0.21	14.55
Fe-Silicate	0.37	2.37
Unclassified	57.57	24.53

Table 3. Nearest Phase Classifications of Black Thunder Ash

Phase	Nearest Phase	%		Mg	Al	Si	Ca	Fe
1	Quartz	3.4	ave	2.0	8.2	76.1	5.6	1.6
			std	7.5	4.3	19.2	7.8	2.8
2	Ca-Aluminate	3.6	ave	11.7	29.8	4.6	45.1	6.5
			std	4.2	2.8	2.9	2.8	2.5
3	Tri Ca-Aluminate	35.4	ave	14.1	21.5	4.7	48.8	7.7
			std	5.5	7.8	3.4	6.8	3.9
4	Gehlenite	4.3	ave	8.9	26.5	12.4	38.4	8.7
			std	4.2	7.6	5.5	5.9	7.5
5	Gehlenite-Na melilite	2.7	ave	5.9	28.2	25.4	28.9	5.4
			std	3.0	4.9	7.8	6.4	5.7
6	Akermanite-Na melilite	5.8	ave	10.7	14.3	30.7	33.7	5.9
			std	7.2	6.9	15.5	7.9	5.8
7	Anorthite	1.3	ave	3.6	37.2	32.1	18.4	3.6
			std	2.4	4.4	5.5	3.9	3.2
8	Plagioclase Solution	25.2	ave	0.6	38.2	50.3	3.3	1.4
			std	1.4	9.7	8.5	4.5	3.4

Table 4. Nearest Phase Classification of Iron Particles in Pittsburgh #8 Ash

Phase	Nearest Phase	%		Na	Mg	Al	Si	S	K	Ca	Fe
1	Gehlenite-Na melilite	0.65	ave	0.8	1.8	23.9	27.4	4.0	0.4	24.8	13.4
			std	1.4	2.1	4.0	7.8	6.8	1.2	6.1	6.6
2	Akermanite-Na melilite	1.35	ave	1.5	5.4	15.0	26.4	3.3	0.1	25.3	17.8
			std	2.0	5.6	4.7	10.2	5.1	0.5	6.6	10.4
3	Anorthite	0.58	ave	0.5	2.1	32.5	34.7	1.8	0.7	15.0	10.3
			std	0.8	2.2	2.6	2.9	3.1	0.9	2.6	3.5
4	Plagioclase	1.2	ave	3.4	2.4	29.0	36.9	4.1	2.1	8.9	10.6
			std	2.7	2.3	4.8	5.5	6.3	1.7	3.5	4.5
5	Kaolinite	2.71	ave	0.7	0.9	21.3	68.1	3.0	1.6	1.2	2.1
			std	1.2	1.7	15.3	18.1	2.9	1.5	1.9	1.8
6	Ca-Al-Silicate	3.66	ave	1.2	4.3	28.4	35.0	1.8	1.1	19.0	5.8
			std	1.5	7.6	9.0	11.2	2.8	1.4	12.9	2.7
7	K-Al-Silicate	2.01	ave	3.9	1.4	31.1	39.8	3.4	7.7	1.3	4.4
			std	4.6	2.4	12.4	14.9	4.7	9.7	2.1	2.9
8	Fe-Al-Silicate	8.99	ave	2.7	2.9	30.0	37.4	1.4	3.2	4.2	15.5
			std	2.1	4.4	7.1	9.0	2.8	2.1	3.4	11.7
9	Iron Silicate	1.76	ave	1.9	1.7	10.9	23.5	4.9	0.6	5.0	49.6
			std	4.5	4.2	7.0	22.6	8.5	1.1	7.9	20.3

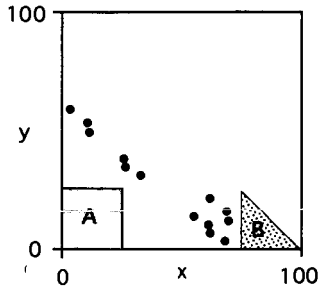


Figure 1. Phases A and B

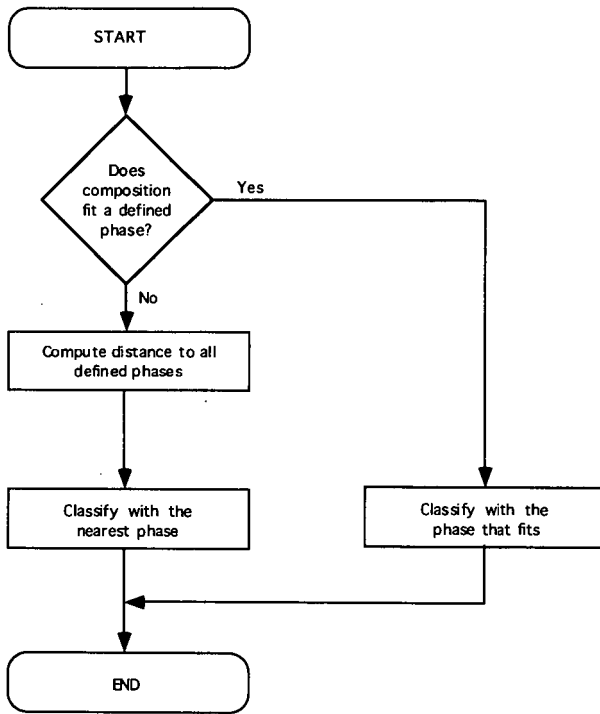


Figure 2. The Algebraic Classification Algorithm